

IMPLEMENTATION OF MASSIVE MIMO IN SUB-6 GHZ AND MMWAVE TECHNOLOGY USING HYBRID PRECODING

K. Sravan Kumar¹, Chillakuru Anusha², Gowrabathina Susmitha², Anala lavanya²,
Gonu Lakshmi Swetha Reddy², Gudimitla Yamini²

¹Associate Professor, Dept. of ECE, Geethanjali Institute of Science and Technology, Nellore, Andhra Pradesh.

²UG Student, Dept. of ECE, Geethanjali Institute of Science and Technology, Nellore, Andhra Pradesh.

Abstract

The massive multiple input multiple output (MIMO) uses arrays with many antennas at the BS to provide vast signal amplification by beamforming and high spatial resolution to multiplex many simultaneous users. Although small-scale MIMO technology has been around for decades, the practical gains have been modest due to the small number of antennas which seldom give sufficient spatial resolution to support many spatially multiplexed streams. Massive MIMO has been demonstrated to achieve an order-of-magnitude higher spectral efficiency in real life, with practical acquisition of channel state information (CSI). 3GPP is steadily increasing the maximum number of antennas in long term evaluation (LTE) and since 64 antennas are supported in Release 15, Massive MIMO has become an integral component of 5G. This work implemented these differences and their implications, while dispelling common misunderstandings. Building on this foundation, we suggest appropriate signal precoding schemes and use cases to efficiently exploit Massive MIMO in both frequencies.

Keywords: massive multiple input multiple output, channel state information, base station, long term evaluation.

1. Introduction

With globalization, present-day networks are facing high traffic demands, and to fulfil these needs, cellular systems are deployed within a few hundred-meter distances, and wireless Local Area Networks (LAN) are placed almost everywhere [1]. Along with increased mobile broadband service, the introduction of new concepts like the Internet of Things (IoT) and Machine-to-Machine Communication (M2M) are also contributing to the increased wireless traffic. The global deployment of cellular service cultivates the cell phone [2] users to be used to the mobile data in their day today life tremendously. The services like video calling, online gaming, social media applications like Facebook, Twitter, WhatsApp, have changed our life drastically with the capabilities of the third generation (3G), fourth generation (4G), and fifth generation (5G) networks, like lower latency and high data rate. A full cell phone connected world is expected in the next few years, which will be mainly characterized by growth in users, connectivity, data traffic volume, and a wide range of applications. In the next few years, technology like [3] augmented reality, virtual reality, ultrahigh definition video, 3Dvideo and features like a mobile cloud will become popular to enrich the ultimate user experience. Massive Multiple-Input Multiple-Output (MIMO) is the most enthralling wireless access technology to deliver the needs of 5G and beyond networks. Massive MIMO is an extension of MIMO technology, which involves using hundreds and even thousands of antennas attached to a base station to improve spectral efficiency and throughput [4]. This technology is about bringing together antennas, radios, and spectrum together to enable higher capacity and speed for the incoming 5G. The

capacity of massive MIMO to increase throughput and spectral efficiency has made it a crucial technology for emerging wireless standards.

The key here is the considerable array gain that massive MIMO achieves with many antennas. Massive MIMO is a key enabling technology for 5G and beyond networks, and as intelligent sensing system primarily rely on 5G and beyond networks to function, massive MIMO and intelligent sensing system are inextricably linked. Massive MIMO systems will perform a crucial role to allow information gathered through smart sensors to be transmitted in real-time [5] to central monitoring locations for smart sensor applications such as an autonomous vehicle, remote healthcare, smart grids, smart antennas, smart highways, smart building, and smart environmental monitoring. 4G mobile networks were introduced in the early 2010s. 4G networks offer data rates up to 100 Mbps and can handle more data traffic [6] with a better quality of service (QoS). 4G networks include applications like video conferencing, online gaming, and mobile television. 4G systems include Worldwide Interoperability for Microwave Access (WiMAX), Long Term Evolution (LTE), and LTE-Advanced (LTE-A), and it has feasible compatibility with older generation networks. The frequency bands of 4G are considerably expensive, and high-end 4G enabled cell phones are required to operate 4G networks. 5G mobile networks are currently starting to be implemented and aim to be 100 times faster than current 4G networks. 5G networks will offer data rates up to 10 Gbps, low latency (in milliseconds), and greater reliability. Imagine that an HD movie can be downloaded in just a few seconds [7]. This technology can support many Internet of Things (IoT) enabled devices and smart vehicles. Efficient wireless access technology that can increase throughput without increasing the bandwidth or densifying the cell is essential to achieve the ongoing demands faced by 5G. 6G mobile networks are complete wireless networks with no limitation. It is currently in the developmental stage, and it will provide incredible transmission speed in the terabit range [8]. This technology would require a smart antenna, large memory in cell phones, and huge optical networks. 6G networks will be cell-free, and it would enable artificial intelligence in wireless networks. It is not clear what frequency band 6G networks will use, but it is apparent that a much higher frequency band will be needed to increase the data rate required for 6G networks [9]. While 5G is supposed to use a frequency greater than 30 GHz and up to 300 GHz (millimeter waves), 6G is associated with much higher frequency in THz bands (300 GHz to 3 THz). The use of the THz spectrum for 6G is estimated to become commercial in the next 5–7 years [10]. Some of the applications for 6G networks are connected robotics and autonomous systems, wireless brain-computer interfaces, blockchain technology, multi-sensory extended reality, space travel, deep-sea sightseeing, tactile internet, and industrial internet. 6G networks are expected to be introduced in the year 2030.

Rest of the paper is organized as follows: Section 2 details about literature survey, section 3 details about the proposed methodology, section 4 details about the results with discussion, and section 5 concludes article with references.

2. Literature Survey

Darwin, R., et al. (2022) [1] proposed a compact massive multi-input multi output (MIMO) antenna system with 1×4 (sector) subarray configuration operating at sub-6 GHz range for 5th generation (5G) base stations has been designed and analysed in various geometries. The capacity of the system can be increased by more than 10 times whereas the energy efficiency can be increased 100 times using the massive MIMO system (Larsson et al. in *IEEE Common Mag* 52(2):186–195, 2014). Buzzi, S., et al. (2022) [12], considered the problem of beam alignment in a cell-free massive MIMO deployment with multiple access points (APs) and multiple user equipments (UEs) simultaneously operating in the same millimeter wave frequency band. Assuming the availability of a control channel

at sub-6 GHz frequencies, a protocol is developed that permits estimating, for each UE, the strongest propagation path from each of the surrounding APs, and to perform user-centric association between the UEs and the APs. Estimation of the strongest paths from nearby APs is realized at the UE in a one-phase procedure, during which all the APs simultaneously transmit on pseudo-randomly selected channels with pseudo-random transmit beamformers. Farasat, Madiha, et al. (2021) [13] They told that mMIMO aims to control the Signal-to-Noise Ratio (SNR) to each user by forming beams to each user unlike single-user MIMO and Multi-User MIMO in LTE and LTE-A. This requires a two-dimensional antenna array with control on the amplitude and phase to steer the beam in azimuth and elevation. Abdullah, Qazwan, et al. (2021) [14] proposed Massive MIMO realizes 5G goals using a large number of antennas. The physical sizes of the antennas are small and inexpensive, which improve both bandwidth and power consumption. Deploying a large number of antennas at the base station (BS) helps to direct the transmission energy into a smaller region of space. With multiple array antennas, objects that were random before tend to be deterministic, which averages out the influence of small-scale fading. Moreover, as the number of BS antennas increases, the random channel vectors between users become orthogonal pair-wise. Millimeter wave communication is also another technology to realize 5G goals. Due to the increased number of users and demand for high data rates, the classic 6 GHz frequency band is depleted. Thereby, the mmWave spectrum, which has a frequency range of 30 - 300 GHz and a wavelength of about 10mm - 1mm. Sharma, Neeraj, et al. (2022) [15]. hybrid precoding architecture, which utilises small size digital precoder followed by large size analog precoder, is employed for such systems. Due to the constant-magnitude hardware constraint on the phase shifter elements of analog precoder, efficient design of hybrid precoders is a challenge. In this paper, a low-complexity non-iterative hybrid precoder/combiner design is proposed for a single-user mmWave massive MIMO system.

Muhammad, et al. (2021) [16]. They proposed that sub-6 GHz BSs not only enhance the network capacity but also improve the energy efficiency of wireless power transfer (WPT). Millimeter wave (MMW) technology features large antenna arrays with high directional beamforming gain and dense base station (BS) deployment that is also beneficial for WPT. Bonfante, et al. (2021) [17]. Reviewed Massive Multiple-Input-Multiple-Output (massive MIMO) and millimeter Wave (mmWave) are key enabling technologies to realize omnipresent, scalable and dynamic 5-th Generation (5G) and beyond networks that provide seamless wireless connectivity supporting enhanced data rates. Fundamental challenges for the full-scale deployments of these technologies are the possibility to integrate different services, e.g, wireless access and backhaul, and the support of applications like industrial robotics demanding a reliable wireless network service. Gunnarsson, S., et al. (2021) [18]. They presented measurement and analysis results for millimeter-wave (mmWave) massive multiple-input multiple-output (MIMO) performance in different real-life scenarios with moderate user equipment (UE) mobility. For the measurement campaign, the developed massive MIMO testbed operating at 28GHz called LuMaMi28GHz is employed. In this testbed, the base station has 16 transceiver chains with a fully digital beamforming architecture (with different pre-coding algorithms) and simultaneously supports multiple users with spatial multiplexing. Nguyen, N. T., et al. (2022) [19]. They investigated hybrid analog-digital beamforming (HBF) architectures for uplink cell-free (CF) millimeter-wave (mmWave) massive multiple-input multiple-output (MIMO) systems. Propose two HBF schemes, namely, decentralized HBF (D-HBF) and semi-centralized HBF (SC-HBF). In the former, both the digital and analog beamformers are generated independently at each AP based on the local channel state information (CSI). In contrast, in the latter, only the digital beamformer is obtained locally at the access point (AP), whereas the analog beamforming matrix is generated at the central processing unit (CPU) based on the global CSI received from all APs. Karad, K. V., et al. (2022) [20]. Proposed a

solution to the effective utilization of band, bandwidth and mapped technologies is the mmWave (millimeter wave) with massive MIMO (multiple inputs multiple outputs). The key factor of 5G technologies is based on mmWave band with antenna array (AA) structure instead antenna compared to microwave communication. It has potential to increase gain, directivity, bandwidth along with spectral efficiency, energy efficiency, handling traffic capacity, enhanced data rate, device to device (D2D) communication, cell coverage and many more.

3. Proposed Methodology

3.1 System Model

In Figure 1, cell 0 UEs correspond to their BS service in the uplink scenario, and cell 0 is interfered with by the UL signals of UEs in cell 1. The average UE-channel gain in cell 0 is B_0^0 , while UE-intrusion in cell channel gain in the average channel

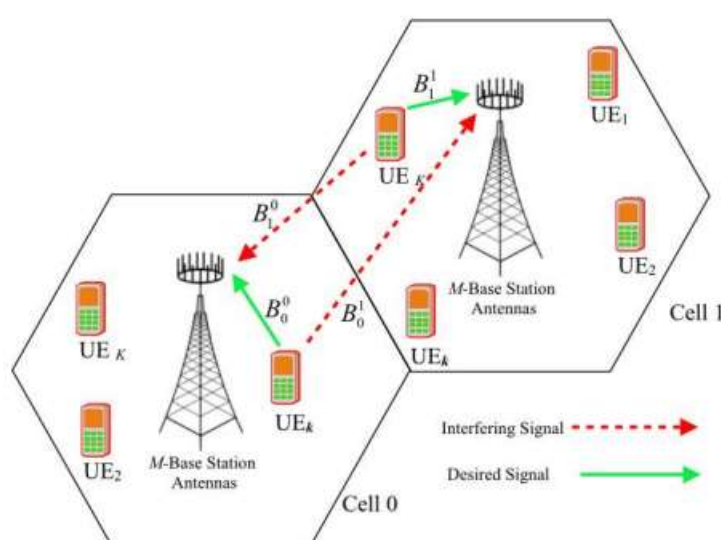


Figure 1. UE to BS system model.

Similarly, cell 1's mean channel gains to its BS operation are B_1^1 , while UE interference signals from cell 0 are on average B_0^1 . The super-script describes the receiving BS cell and the cell in which the subscript designates the transmitting UE lives. The average channel gains are positive, often minimal, dimensional amounts because signal energies easily fall off with the distance of propagation. In the cell serving, values of -70dB to -120 dB are predicted, although fewer are expected for signals that intervene.

To conclude, inflating the propagation capacity of the SNR extends the SE, but the excellent outcome quickly transfers the network to a device with no extraordinary interruption. It is primarily attributed to a lack of the degree of freedom at the base station, and the signal attempted by the signal interaction with measurements can't not be recognized. The interference-limited device operates in existing networks, while the hotspot level is dependent on the use of BSs.

At first, no pilot contamination at various base stations N is assumed to be $\{128, 256\}$ and treated as $B=1$. And, we use the separate mixture order L belong to $\{2, 3, 5\}$ and the results are elevated on the pilots' random sequences. As the mixing order L is increased, the simulation figures decrease the MSE of the Bayesian estimator.

3.2 Proposed Method

The system model for massive MIMO systems based on OFDM has been first introduced. Then some new pilot overhead reduction research on large MIMO-OFDM systems is discussed. Fig. 2, where the BS reputed to have M transmitting antennas and serving K individual single- antenna users ($K \ll M$) with N OFDM tones, is the large MIMO device model Downlink-Scenario. In reality the number of tones available is split between and, where the tones in set is used to transmit data and to the guard band is used in its complementary set. The corresponding $K \times 1$ vector is then for each tone \in , consisting of symbols for K users, normally selected by a complex signal B alphabet.

To satisfy the requirements of $\|s\| = 1$. We normalize the data vector. We sent $s = o \times$ for each tone \in , so that we didn't transmit any signals in the guard band. Since a supportive user identification is often not feasible, BS precoding is needed to prevent multiple users' interference (MUI). In the i th tone, the signal vector is generally precoded linearly with $=$. Where $\in \square \times$ is a preceded vector containing symbols emitted by an M antenna on the n th subcarrier, and $\in \square \times$ is a precoding matrix in the n th OFDM tones, respectively. Two classical pre-coding systems are zero-forcing (ZF) precoding and MMSE pre-coding [83].

The first seeks to remove the MUI, the last balancing the annulment of the MUI with improved noise. The ZF precoding system is considered in this chapter since $K \ll M$, has an infinite range of forms, the ZF precoding matrix, which is the most commonly used one which is $= ()$. Where $\in \square \times$ refers to the i th tone-related channel matrix of MIMO. Here we conclude that the, ostensibly known channel matrix, is known to the transmitter by using the time-division duplexing (TDD) reciprocity systems.

Both pre-coded vectors are reorganized into M antennas for OFDM modulation after pre-coding, $[s_1, \dots, s_M]^T = [s_1, \dots, s_M]^T$, where $\in \square \times$ is the frequency domain signal from the m th antenna broadcast. In IDFT, i.e., $= \mathcal{V}$, the time domain signals are received. To avoid inter-symbol interferences, a cyclic prefix is used for the time-domain samples for each antenna. Finally, the samples are transferred and distributed through a selective frequency channel to analog signals.

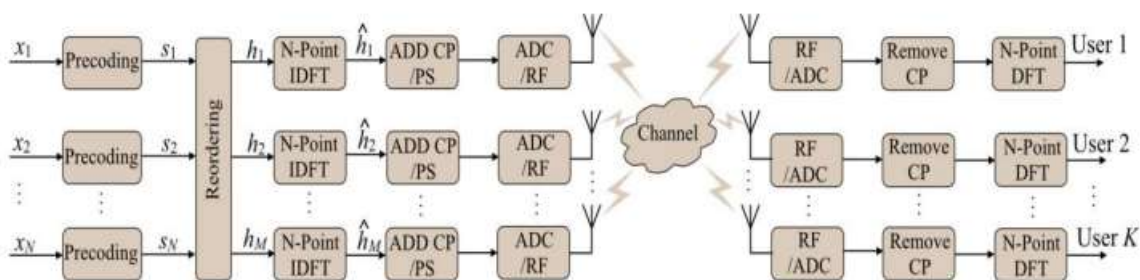


Figure 2. System model for the downlink OFDM-based massive MIMO.

The DFT is conducted for frequency-domain signals after CPs have been removed from the receiver signal. The obtained received vector of K users' signals as $= +, \mathcal{V}$. Denotes the obtained vector of the i th tone and $\in \square \times$ is a noise from the recipient and i.i.d circularly symmetrical, Gaussian input of a zero mean and variance. When the ZF pre-coding system is used, the signal vector obtained is equal to $= +, \mathcal{V}$, so the MUI is extracted perfectly.

Choosing Between Analog, Hybrid, and Digital Beamforming

The number of channel coefficients grows linearly with the number of antennas at the BS and UE. To have an approximate idea of the computational burden, consider a system with 200 BS antennas and

20 spatially multiplexed single-antenna UEs. Consider OFDM with 1024 subcarriers and channels that are constant over 12 subcarriers. There are $3.4 \cdot 10^5$ complex scalar coefficients, which amounts to $6.8 \cdot 10^6$ estimates/second if a channel coherence time of 50 ms is assumed. These numbers increase if there are more antennas, more subcarriers, and/or shorter coherence time. At sub-6 GHz, there is generally multi-path propagation caused by a multitude of scattering clusters. The channel coefficients are correlated across antennas, but this can only be utilized to marginally improve the estimation quality, at the cost of substantially higher complexity [5, Sec. 3]. Nevertheless, the estimation can be conveniently implemented/parallelized in hardware [9] and the estimation overhead is small when operating in time-division-duplex (TDD) mode and exploiting channel reciprocity to only send uplink pilots [4]. At mmWave, the channel can potentially be parameterized (considering a phase-synchronized array with a known angular array response) because it consists of a (potential) LoS path and few one-bounce reflections.

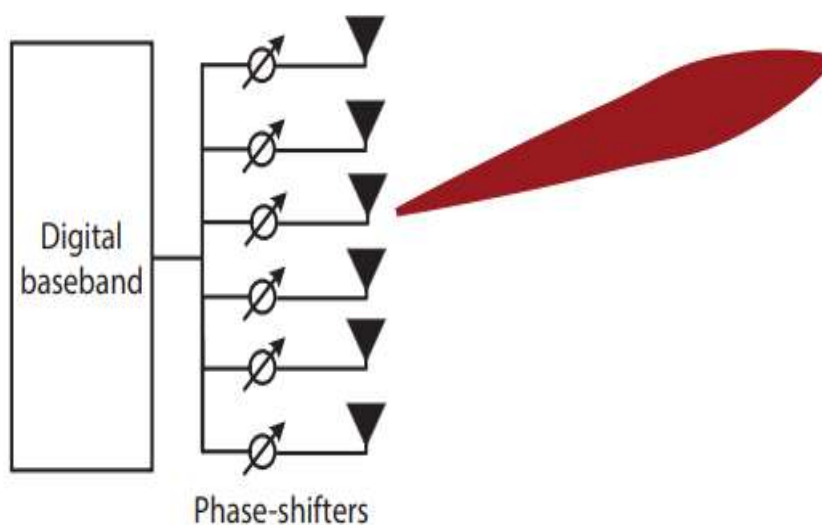
Instead of estimating the individual channel coefficients, a few angular channel coefficients can be estimated to acquire the entire channel, leading to greatly reduced complexity. When a single data-stream is to be sent, it is The number of channel coefficients grows linearly with the number of antennas at the BS and UE. To have an approximate idea of the computational burden, consider a system with 200 BS antennas and 20 spatially multiplexed single-antenna UEs. Consider OFDM with 1024 subcarriers and channels that are constant over 12 subcarriers. There are $3.4 \cdot 10^5$ complex scalar coefficients, which amounts to $6.8 \cdot 10^6$ estimates/second if a channel coherence time of 50 ms is assumed. These numbers increase if there are more antennas, more subcarriers, and/or shorter coherence time. At sub-6 GHz, there is generally multi-path propagation caused by a multitude of scattering clusters. The channel coefficients are correlated across antennas, but this can only be utilized to marginally improve the estimation quality, at the cost of substantially higher complexity. Nevertheless, the estimation can be conveniently implemented/parallelized in hardware [9] and the estimation overhead is small when operating in time-division-duplex (TDD) mode and exploiting channel reciprocity to only send uplink pilots [4]. At mmWave, the channel can potentially be parameterized (considering a phase-synchronized array with a known angular array response) because it consists of a (potential) LoS path and few one-bounce reflections. Instead of estimating the individual channel coefficients, a few angular channel coefficients can be estimated to acquire the entire channel, leading to greatly reduced complexity. When a single data-stream is to be sent, it.

Choosing Between Analog, Hybrid, and Digital Beamforming

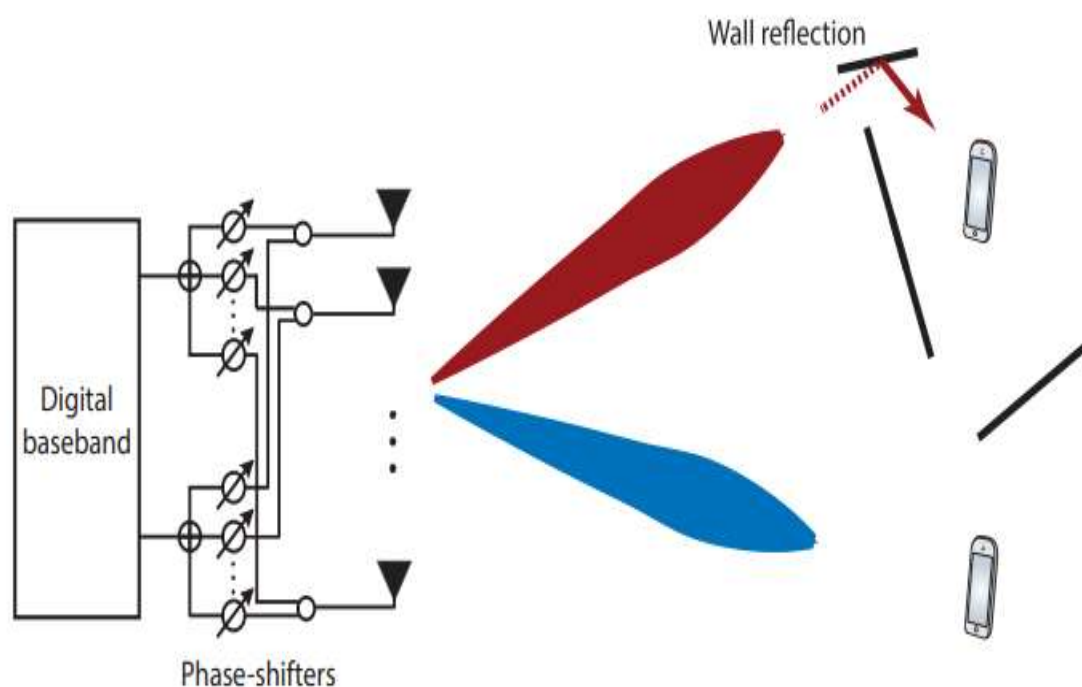
Current hardware can realize full digital beamforming at sub-6 GHz, while hybrid analog/digital beamforming is a potential design-simplification at mmWave. With analog transmit beamforming, a phase-shifted version of the same signal is transmitted from all antennas. This leads to a signal beam directed in a particular angular direction (see Fig. 3a). If multiple UEs are multiplexed, one set of analog phase-shifters (connected to a separate input from the baseband) is needed per UE (see Fig. 3b). This is hybrid beamforming in a nutshell. The number of UEs cannot be larger than the number of baseband-inputs, but digital precoding can be used to assign a mix of the UEs' signal to each input. In contrast, full digital beamforming can send any signal from any antenna. This flexibility can be exploited at sub-6 GHz frequencies to deliver high beamforming gain in rich multi-path environments, as illustrated in Fig. 3c.

The digital flexibility is evident in multi-user scenarios, where the antennas should transmit a superposition of many beams per UE, different beams per subcarriers (due to frequency-selective fading), and multiplex many UEs on the same time-frequency resource slot. Analog beamforming cannot adapt the beam to multipath propagation and frequency-selective fading, while hybrid

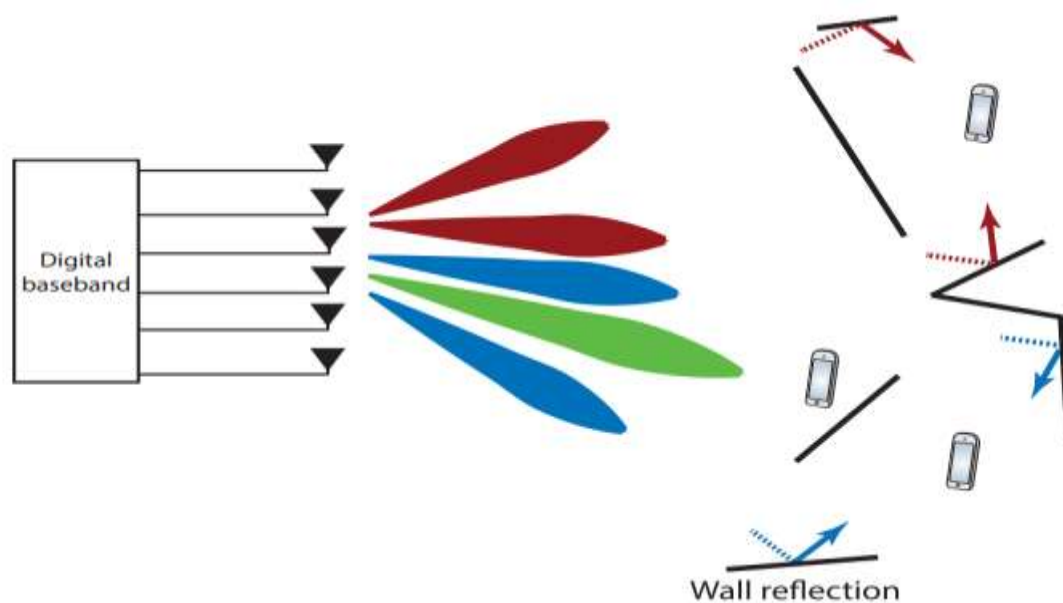
beamforming has only a limited ability to do that since the phase-shifters create a set of fixed beams that the digital precoding needs to be based on. mmWave systems have lower user multiplexing capability if implemented with hybrid beamforming, since the number of UEs is limited by the number of sets of phase-shifters. However, even analog beamforming (Fig. 3a) suffices for single-user communications over wide bandwidths. To illustrate this fact, we consider a LoS channel with five reflections. The center frequency is 60 GHz and we use the method in [5, Sec. 7.3.2] to compute the array response for different frequencies. We consider 32×32 , 64×64 , and 128×128 planar arrays with half-wavelengthspaced antennas. The maximum beamforming gain is equal to the number of antennas and is achievable by digital beamforming. Figure 4 shows the percentage of the maximum beamforming gain that is obtained by analog beamforming at different frequencies around the center frequency. It starts at 90 percent since no analog beamforming matches the array response when there are reflections. Nevertheless, if the bandwidth is 400 MHz, 80–90 percent of the maximum beamforming gain can be achieved in the entire band by analog beamforming. If the bandwidth continues to grow, the beamforming gain drops since the beamforming is optimized for the center frequency. This is known as the beam-squinting effect. The gain loss is particularly severe for larger arrays, since the beams are narrower. With the 32×32 array, more than 75 percent of the maximum gain can be achieved over a 2 GHz bandwidth, while the gain drops quickly for the 128×128 array.



- (a) **Analog beamforming:** Only one beam is created for the entire frequency band, which is sufficient for LoS beamforming.



(b) **Hybrid beamforming:** A few beams are created by the analog phase-shifters and the digital baseband can create superpositions of these beams to adapt to multi-path and frequency-selective fading, which gives a limited exibility for handling NLoS scenarios.



(b) **Digital beamforming:** Full exibility to create a superposition of any number of beams and adapt the beams to multi-path and frequency-selective fading.

Figure 3. The hardware implementation of beamforming determines the flexibility in handling difficult propagation scenarios, which in turn has implications on the use cases. The system is viewed

from above and different colors represent different signals: a) analog beamforming; b) hybrid beamforming; and c) digital beamforming.

4. Results and Discussion

The maximum beamforming gain is equal to the number of antennas and is achievable by digital beamforming. Figure 4 shows the percentage of the maximum beamforming gain that is obtained by analog beamforming at different frequencies around the center frequency. It starts at 90 percent since no analog beamforming matches the array response when there are reflections. Nevertheless, if the bandwidth is 400 MHz, 80–90 percent of the maximum beamforming gain can be achieved in the entire band by analog beamforming. If the bandwidth continues to grow, the beamforming gain drops since the beamforming is optimized for the center frequency. This is known as the beam-squinting effect. The gain loss is particularly severe for larger arrays, since the beams are narrower.

With the 32×32 arrays, more than 75 percent of the maximum gain can be achieved over a 2 GHz bandwidth, while the gain drops quickly for the 128×128 array.

The phases are selected to maximize the inner product with the array response at the center frequency.

There is a LoS path with azimuth angle $\pi/4$ and elevation angle $-\pi/4$ to the array, measured from the boresight.

There are also five reflections, with the azimuth angles $\pi/6, \pi/3, \pi/4, \pi/4, \pi/12$ and the corresponding elevation angles $-\pi/5, -\pi/5, -\pi/6, -\pi/12, \text{ and } -\pi/6$. The total gain of the LoS equals the gain of all the reflections.

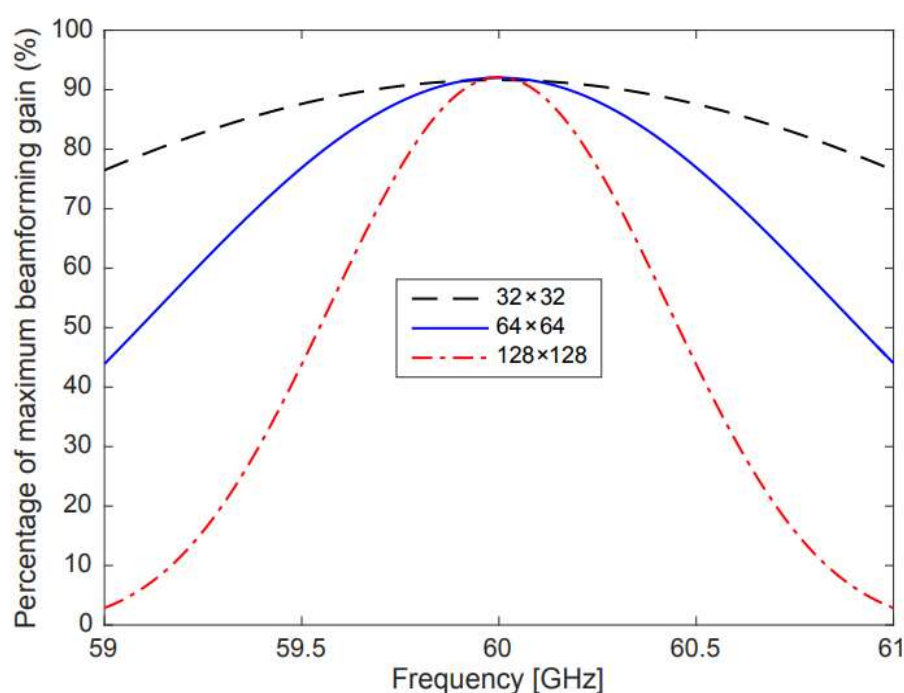


Figure 4. The fraction of the maximum beamforming gain that is achieved at different frequencies when analog beamforming is used.

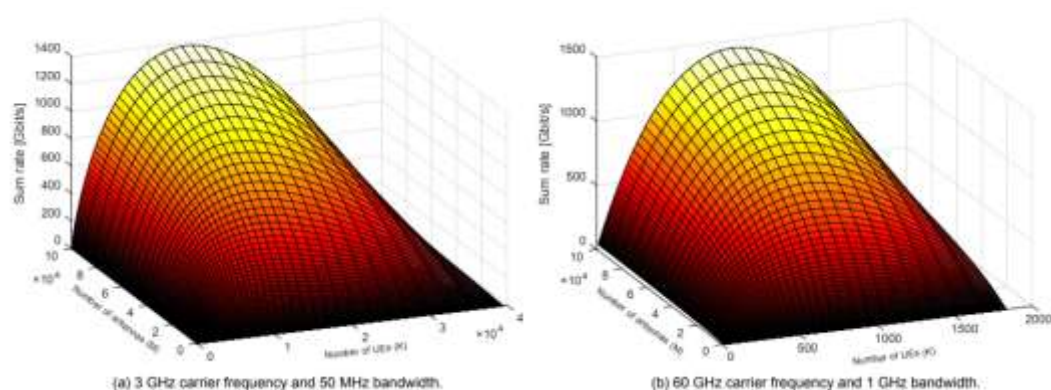


Figure 5. Downlink sum rate that is achieved when operating at different carrier frequency's using TDD and digital beamforming, as a function of the number antennas.

Figure 5 shows the downlink sum rate when operating at these frequencies, as a function of the number of antennas and UEs, and assuming that fully digital reciprocity-based beamforming is used in all cases. The sum rate grows monotonically with the number of antennas, as expected. The highest values on the curves are 1.38 Tb/s at 3 GHz (with 50 MHz bandwidth) and 1.44 Tb/s at 60 GHz (with 1 GHz bandwidth), which are nearly the same. The huge difference is that the peak values are achieved by multiplexing 14,000 or 870 UEs, respectively. This corresponds to allocating 35 percent and 44 percent of the coherence blocks to uplink pilots, respectively. The mmWave setup delivers 1.66 Gb/s per UE, while the sub-6 GHz setup only delivers 99 Mb/s per UE but compensates by serving extremely many UEs. This exposes the fundamental operational difference; the huge bandwidth in mmWave bands allows for high per-UE rates, while the longer coherence time at sub-6 GHz allows for spatial multiplexing of more UEs.

Which solution is preferable depends on the data traffic characteristics of the future, but why not deploy both? The maximum number of antennas was 100,000 in this futuristic simulation. Assuming 3 GHz and half-wavelength-antenna-spacing, these antennas can be deployed in array of 31 m \times 31 m. At 60 GHz, this shrinks to 1.58 m \times 1.58 m. Both setups can easily be deployed at the face of a skyscraper, so the size is not an issue. However, adequate implementation strategies are needed to cope with bottlenecks in connecting and processing the many signals.

The uplink SNR to each receive-antenna is 20 dB when operating at 3 GHz with 50 MHz bandwidth and scaled accordingly when operating at 60 GHz with 1 GHz bandwidth to keep the transmit power fixed. The downlink transmission uses 100 times more power than the uplink pilot transmission. Closed-form rate expressions from [4, Sec. 3.3] were used to generate the figures. To make the signal processing complexity scalable, maximum ratio transmission and channel estimation based on uplink pilots are assumed. a) 3 GHz carrier frequency and 50 MHz bandwidth; b) 60 GHz carrier frequency and 1 GHz bandwidth.

5. Conclusion

This work has reviewed the major differences in mMIMO design for sub-6 GHz and mmWave frequencies, concerning the propagation mechanisms, transceiver hardware, and signal processing algorithms. The impact on the various envisioned 5G use-cases has been explained, showing that both bands offer attractive propositions. Computational complexity is no longer a main bottleneck, but less considered factors, such as the interconnect of signals, both for central baseband processing and at mmWave to antennas, constitute potential bottlenecks. The technology is at a more advanced stage at sub-6 GHz, yet challenges exist in both bands. Several intriguing questions remain unanswered: Will

mmWave mMIMO be implemented with full digital beamforming? Which mMIMO features will be actually used in 5G networks? Will the multiplexing capabilities ever be pushed as high as illustrated in the Central Park example? How will data-traffic patterns and applications evolve? Whatever the answers will be, mMIMO will certainly play a paramount role in the shaping of future wireless networks in both bands.

While this article has substantiated how mMIMO offers unprecedented performance to end users, other applications are envisioned, such as the implementation of cloud-RAN through in-band wireless fronthauling. The enormous amount of baseband data available in mMIMO systems can be also used to sense the environment; for example, estimate the amount of traffic on a road, count the number of persons in a room, or guard against intrusion in protected spaces. In conclusion, as far as mMIMO is concerned, the best is yet to come.

References

- [1] Chen, W., Lv, G., Liu, X., Wang, D., & Ghannouchi, F. M. (2020). MIMO Energy-efficient integrated DPA MMICs for sub-6-GHz and mm-wave 5G massive MIMO systems. *IEEE Microwave Magazine*, 21(5), 78-93.
- [2] Inoue, A. (2021). Millimeter-wave GaN devices for 5G: massive MIMO antenna arrays for sub-6-GHz and mm-wave bandwidth. *IEEE Microwave Magazine*, 22(5), 100-110.
- [3] Pfadler, A., Ballesteros, C., Romeu, J., & Jofre, L. (2020). Hybrid massive MIMO for urban V2I: Sub-6 GHz vs mmWave performance assessment. *IEEE Transactions on Vehicular Technology*, 69(5), 4652-4662.
- [4] Aerts, S., Verloock, L., Van Den Bossche, M., Colombi, D., Martens, L., Törnevik, C., & Joseph, W. (2019). In-situ measurement methodology for the assessment of 5G NR massive MIMO base station exposure at sub-6 GHz frequencies. *IEEE Access*, 7, 184658-184667.
- [5] Sam, Leen, Matthias Van Den Bossche, Davide Colombi, Luc Martens, Christer Törnevik, and Wout Joseph. "In-situ measurement methodology for the assessment of 5G NR massive MIMO base station exposure at sub-6 GHz frequencies." *IEEE Access* 7 (2019).
- [6] Jaglan, N., Gupta, S. D., & Sharawi, M. S. (2021). 18 elements massive MIMO/diversity 5G smartphones antenna design for sub-6 GHz LTE bands 42/43 applications. *IEEE Open Journal of Antennas and Propagation*, 2, 533-545.
- [7] Ishteyaq, I., & Muzaffar, K. (2022). Multiple input multiple output (MIMO) and fifth generation (5G): An indispensable technology for sub-6 GHz and millimeter wave future generation mobile terminal applications. *International Journal of Microwave and Wireless Technologies*, 14(7), 932-948.
- [8] A., Ballesteros, C., Romeu, J., & Jofre, L. (2020). Hybrid massive MIMO for urban V2I: Sub-6 GHz vs mmWave performance assessment. *IEEE Transactions on Vehicular Technology*.
- [9] Insha, and Khalid Muzaffar. "Multiple input multiple output (MIMO) and fifth generation (5G): An indispensable technology for sub-6 GHz and millimeter wave future generation mobile terminal applications." *International Journal of Microwave and Wireless Technologies* 14.7 (2022): 932-948.

- [10] Jabeen, S., & Khan, Q,U,(2022). An integrated MIMO antenna design for Sub-6 GHz & millimeter-wave applications with high isolation. *AEU-International Journal of Electronics and Communications*, 153, 154247.
- [11] Darwin, R., & Sampath, P. (2022). Sub-6 GHz band massive MIMO antenna system for variable deployment scenarios in 5G base stations. *Microsystem Technologies*, 28(9), 2047-2059.
- [12] Buzzi, S., D'Andrea, C., Fresia, M., & Wu, X. (2022). Multi-UE Multi-AP Beam Alignment in User-Centric Cell-Free Massive MIMO Systems Operating at mmWave. *IEEE Transactions on Wireless Communications*, 21(11), 8919-8934.
- [13] Farasat, Madiha, Dushmantha N. Thalakituna, Zhonghao Hu, and Yang Yang. "A review on 5G sub-6 GHz base station antenna design challenges." *Electronics* 10, no. 16 (2021): 2000.
- [14] Abdullah, Qazwan, Adeb Salh, Nor Shahida MohdShah, Noorsaliza Abdullah, Lukman Audah, Shipun Anuar Hamzah, Nabil Farah, Maged Aboali, and Shahilah Nordin. "A brief survey and investigation of hybrid beamforming for millimeter waves in 5G massive MIMO systems." *arXiv preprint arXiv:2105.00180* (2021).
- [15] Sharma, Neeraj, and Bhasker Gupta. "Low-complexity non-iterative hybrid precoding scheme for millimeter wave massive MIMO systems." *International Journal of Electronics* 109, no. 3 (2022): 410-426.
- [16] Muhammad, N. A., Seman, N., Apandi, N. I. A., & Li, Y. (2021). Energy harvesting in sub-6 GHz and millimeter wave hybrid networks. *IEEE Transactions on Vehicular Technology*, 70(5), 4471-4484.
- [17] Bonfante, A. (2021). *Massive MIMO and Millimetre Wave Technologies: Design, Application and Integration with ML Techniques for 5G and Beyond Networks* (Doctoral dissertation, Trinity College Dublin. School of Engineering. Discipline of Electronic & Elect. Engineering).
- [18] Gunnarsson, S., Chung, M., Johansson, A., Liu, L., Tufvesson, F., Edfors, O., ... & Clifton, C. (2021). mmWave Massive MIMO in Real Propagation Environment: Performance Evaluation Using LuMaMi28GHz. In *2021 55th Asilomar Conference on Signals, Systems, and Computers* (pp. 80-84). IEEE.
- [19] Nguyen, N. T., Lee, K., & Dai, H. (2022). Hybrid beamforming and adaptive RF chain activation for uplink cell-free millimeter-wave massive MIMO systems. *IEEE Transactions on Vehicular Technology*, 71(8), 8739-8755.
- [20] Karad, K. V., & Hendre, V. S. (2022). Review of antenna array for 5G technology using mmwave massive MIMO. In *Recent Trends in Electronics and Communication: Select Proceedings of VCAS 2020* (pp. 775-787). Springer Singapore.